International Journal of Electrical and Computer Engineering (IJECE)
Vol. 14, No. 2, April 2024, pp. 1594~1603
ISSN: 2088-8708, DOI: 10.11591/ijece.v14i2.pp1594-1603

An automated system for classifying types of cerebral hemorrhage based on image processing techniques

Areen Arabiat, Muneera Altayeb
Department of Communications and Computer Engineering, Faculty of Engineering, Al-Ahliyya Amman University, Amman, Jordan

Article Info

Article history:

Received Nov 18, 2023
Revised Dec 29, 2023
Accepted Jan 5, 2024

Keywords:

Brain computed tomography images
Convolutional neural networks
K-nearest neighbors
Logistic regression
Orange3 data mining
Support vector machine

ABSTRACT

The brain is one of the most important vital organs in the human body. It is responsible for most of the body's basic activities, such as breathing, heartbeat, thinking, remembering, speaking, and others. It also controls the central nervous system. Cerebral hemorrhage is considered one of the most dangerous diseases that a person may be exposed to during his life. Therefore, the correct and rapid diagnosis of the hemorrhage type is an important medical issue. The innovation in this work lies in extracting a huge number of effective features from computed tomography (CT) images of the brain using the Orange3 data mining technique, as the number of features extracted from each CT image reached (1,000). The proposed system then uses the extracted features in the classification process through logistic regression (LR), support vector machine (SVM), k-nearest neighbor algorithm (KNN), and convolutional neural networks (CNN), which classify cerebral hemorrhage into four main types: epidural hemorrhage, subdural hemorrhage, intraventricular hemorrhage, and intraparenchymal hemorrhage. A total of (1,156) CT images were tested to verify the validity of the proposed model, and the results showed that the accuracy reached the required success level with an average of (97.1%).

Corresponding Author:

Areen Arabiat
Department of Communications and Computer Engineering, Faculty of Engineering, Al-Ahliyya Amman University
Al-Salt, Amman, Jordan
Email: a.arabiat@ammanu.edu.jo

1. INTRODUCTION

Accurate and rapid diagnosis and identifying the location and type of hemorrhage in computed tomography (CT) images are critical steps in the patient's treatment. The diagnosis requires urgent intervention. When a patient is presented with acute neurological symptoms such as severe headaches or loss of consciousness, highly trained specialists examine medical images of the patient's brain to identify the presence, location, and type of hemorrhage of intracranial hemorrhages (ICHs). This is an important area of medicine. It was noted that the rate of infection with this disease has reached 25 per 100,000 people per year [1]–[3]. Therefore, the correct and fast diagnosis of the presence of hemorrhages and the classification of the type of hemorrhage is essential to helping the patient recover and reduce the severity of the disease. Several researchers in the literature have studied ICHs by analyzing, locating, and classifying the hemorrhage in samples from patients' CT images. The purpose was to assist doctors in the early diagnosis and accurate identification of the type of hemorrhage. Computer-aided detection (CAD) systems rely on a combination of powerful machine learning algorithms and the abundant and diverse data that can be collected from these contemporary tools. Recent years have seen the inclusion of CAD into regular clinical practice to identify a few serious diseases, including breast and lung cancer, due to its potential for effective support. Furthermore, CAD has gradually emerged as a prominent field of study in the area of diagnostic radiology and medical imaging [4], [5].

Sage and Badura [6] introduced a method for identifying various sorts of cerebral hemorrhages in head computed tomography images. Each hemorrhage subtype's trained model is built using a double-branch convolutional neural network with ResNet-50 architecture. Features are extracted from two chromatic presentations of the input data: a stack of three successive slices that creates a three-dimensional spatial context, and a concatenation of the image normalized in different intensity windows. To arrive at the ultimate choice, the classifier receives the combined feature vector. The random forest and the support vector machine were the two tools we tested. 372,556 images from 11,454 CT series of 9,997 patients were used in the tests, and labels about the different hemorrhage subtypes were labeled on each image. They verified the model using either of the two classifiers under consideration, as well as deep networks from both branches of our architecture. The outcomes obtained support the random forest classifier's employment in conjunction with a variety of double-source characteristics. The accuracy of the algorithm performance achieved for intraventricular hemorrhage (96.7%) and intraparenchymal hemorrhage (93.3%). In Nemcek *et al.*'s work [7], a convolutional neural network was used to detect and classify ICHs, including localization, where the localization and classification algorithm of the type of ICHs was based on the analysis of two-dimensional orthogonal tomography slices. The slice has been analyzed by four binary convolutional neural networks (CNN) classifiers, which determine the presence or absence of the specific type of hemorrhages in the slice, except the extradural haematoma (EDH), which has a low occurrence in the tested sample, this system achieved an average classification accuracy of 53.7% [7].

Okuyar and Kamanli [8] have used deep learning as a sophisticated approach to detect strokes in medical imaging. Deep learning models, CNNs, have shown potential in detecting strokes using CT images. These models can learn to recognize patterns in images that indicate a stroke, such as the presence of an infarct or hemorrhage. one deep learning model example is U-Net, which is extensively used for medical image segmentation, and is employed for stroke identification in CT images. CNNs have been trained to classify brain CT scans as normal or abnormal. The goal of this study is to determine whether a stroke is occlusive (ischemic) or hemorrhagic (hemorrhagic) based on brain CT images taken without the use of a contrast agent. The performance of different classification models was compared, with the convolutional neural network with 16 layers deep (VGG-16) achieving a success rate of 94%. Moreover, the U-Net model achieved a 60% score, effectively discerning discrepancies between ischemic and hemorrhagic strokes [8]. Gudadhe and Thakare [9] developed a hybrid feature selection approach to extract a common feature vector from CT images by applying discrete wavelet transforms (DWT), discrete cosine transforms (DCT), and gray-level co-occurrence matrixes (GLCM) in a CT image. The CT images of intracranial hemorrhage are then classified by running random tree, random forest, and REP-Tree machine learning algorithms. The classification results showed that the highest accuracy was for the random forest classifier, which reached 87.97% for the DWT and GLCM feature sets [9]. The novelty of this work lies in using Orange3 as a new data mining method to extract a huge number of efficient features from CT images of patients with cerebral hemorrhage and employing these features in the cerebral hemorrhage classification process by applying four classification algorithms: logistic regression (LR), convolutional neural networks (CNN), support vector machine (SVM), and k-nearest neighbor algorithm (KNN).

2. METHOD

The proposed classification model relies on the extraction of features from the CT images using a new data mining tool after applying an image enhancement process using Python as a preprocessing stage to improve the quality and appearance of an image. This step is used to increase the efficiency of the feature extraction process, which is used later in the classification process, as shown in Figure 1. The feature extraction procedure was implemented using a deep learning model within the Orange3 data mining software, and then the extracted feature victors of CT images were subjected to classification using four distinct classifiers to distinguish between four classes of cerebral hemorrhage; epidural, intraparenchymal, intraventricular, and subdural hemorrhage. The classifiers applied in this study encompassed LR, CNN, SVM, and KNN. Model evaluation was performed utilizing a 10-fold cross-validation methodology. The results were compared to determine the algorithm that demonstrated the most effective performance for image classification tasks, as described in Figure 2.

2.1. Dataset

The registered open dataset Kaggle [10], which was used in this study consists of CT brain scans with cerebral hemorrhage. Each image represents a detail of a patient's brain taken using CT, with a total number of 1,156 images. A sample of cerebral CT images is shown in Figure 3.

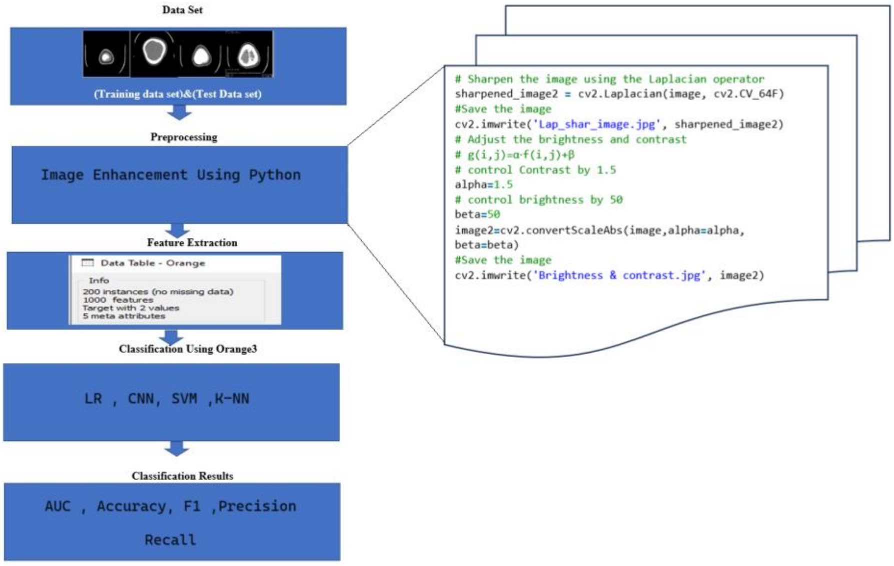

Figure 1. The proposed model

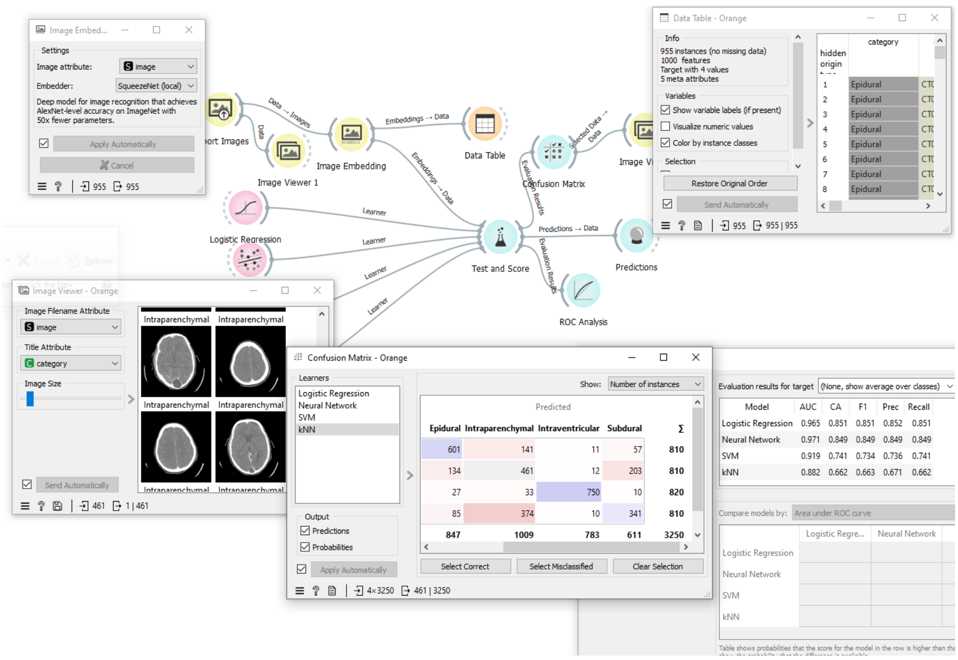

Figure 2. Orange3 software model

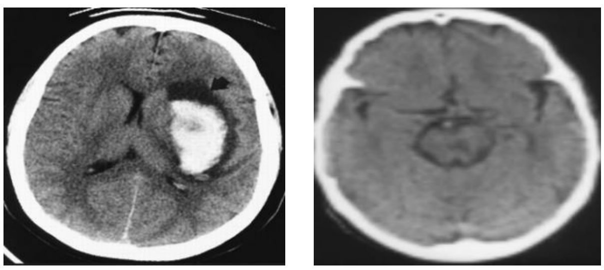

(a) (b)

Figure 3. Brain CT images (a) no hemorrhage, (b) hemorrhage [10]

The dataset is distributed, and the model is validated using k-fold cross-validation. We utilize = 10, which indicates that the data will be split into ten folds (F1, F2, F3, …, F10) for each class. To provide a representative sample, Figures 4(a) to (d) show a subset of cerebral hemorrhage CT images (epidural, intraparenchymal, intraventricular, and subdural).

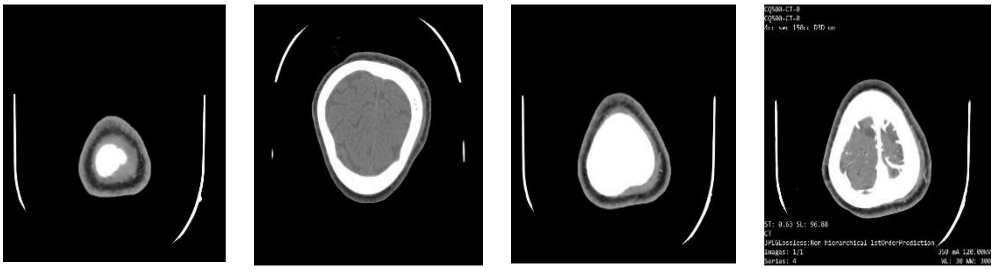

(a) (b) (c) (d)

Figure 4. Cerebral hemorrhage CT images, (a) epidural (b) intraparenchymal, (c) intraventricular, (d) subdural [10]

2.2. Classification methods

Machine learning, a discipline within computer science, encompasses a wide range of techniques aimed at empowering computers to acquire knowledge and enhance their performance through learning mechanisms, without the necessity of explicit programming. Its primary objectives and applications revolve around tasks such as prediction and optimization, where machines are empowered to analyze data and make informed decisions based on patterns and insights derived from the data. In our study, we employed several supervised classification methods. In the following sections, an explanation of each classification method utilized in this research [11].

2.2.1. Logistic regression (LR)

Logistic regression (LR) is a commonly used research method in the health sciences to determine the occurrence of an event, especially in disease states and decision-making scenarios. Unlike assuming a linear relationship, LR connects the logit of the outcome with predictor values. In LR, the dependent variable must be categorical, while the independent variables do not need to meet specific requirements, such as being interval variables or normally distributed. The categories used in LR should be mutually exclusive and exhaustive. LR is widely used in the fields of large-scale data and machine learning for data classification. In this approach, the optimal parameters of the loss function, which possess a certain level of convexity, are determined using the gradient descent method [12]. This form of statistical model is commonly used in categorization and predictive analytics. Logistic regression determines the probability that an event, such as voting or not voting, will occur based on a collection of independent factors. Since the outcome is a probability, the range of the dependent variable is 0 to 1. The logit formula is used in logistic regression to translate the odd, which is the likelihood of success divided by the probability of failure. This logistic function, often known as the log odds or the natural logarithm of odds, is represented by (1) and (2):

$$Logit(Pi) = \frac{1}{(1+\exp(-pi))} \tag{1}$$

$$\ln\left(\frac{pi}{(1-pi)}\right) = \beta_0 + \beta_1 * X_1 \ldots . + \beta_k * X_k \tag{2}$$

In this logistic regression equation, x is the independent variable, and logit (pi) is the dependent or response variable. The beta parameter or coefficient in this model is often estimated using maximum likelihood estimation (MLE) [13].

2.2.2. k-nearest neighbor (KNN)

A supervised machine learning method for classification, the KNN algorithm, is very useful for predicting diseases. Using the features and labels from training data, it makes predictions about the categorization of unlabeled data and then utilizes a majority voting procedure to determine the final classifications by choosing 'k' number of unique clusters, k-nearest neighbor divides the data into spherical clusters, and then locating a set of cluster centers by looking at the cluster labels of a particular data point's k

closest neighbors in the training data, this method may identify the cluster for that data point [14]. A predetermined distance metric, or Euclidean distance metric, is used to identify the neighbors. Equation (3) is used to get the sum of errors (SSE) by computing the common Euclidean distance between each cluster center and the point [15].

$$SSE = \sum_{i=1}^{k} \sum_{x \in C_i} dist^2 (m_i, x) \tag{3}$$

In the context where x represents a data point residing in cluster C_i, k denotes the number of clusters, m_i signifies the center (mean) of the cluster, and distance refers to the Euclidean distance [16].

2.2.3. Support vector machine (SVM)

Support vector machines (SVMs) are state-of-the-art classifiers and are a class of supervised learning models that employ associated learning algorithms to analyze data for classification and regression analysis. The primary function of SVMs is to delineate decision boundaries, referred to as boundaries, to separate different classes within the dataset [17]. These boundaries are constructed in such a way that the distance between the boundaries and the classes is maximized, leading to the minimization of classification errors. In essence, SVMs aim to optimize the margin separation to enhance the accuracy of classification. More specifically, in the context of machine learning, a learning algorithm utilizes a given dataset consisting of input data and their corresponding known responses (classes) to train a model as described in Figure 5. The objective is to enable the model to make dependable predictions about the behavior or outcome of new, unseen data [18], [19].

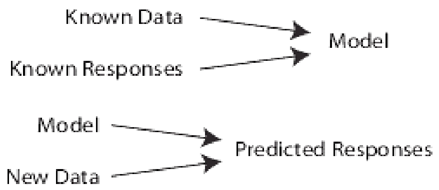

Figure 5. Description of SVM [16]

2.2.4. Convolutional neural network (CNN)

Convolutional neural networks (CNN) are used in automatic image categorization systems [20]. In most situations, we use features from the top layer of CNN for classification; nevertheless, such features may not include enough valuable information to properly forecast an image. The convolutional layer is the layer that can extract features from pictures. Convolution keeps the link between distinct regions of an image since pixels are only connected to neighboring and near pixels [21], [22]. Several various nodes or neurons connected form a neural network, which is an operational model. Each node in the model serves as a processing function, and weights are used to indicate connections between nodes to simulate an artificial neural network's memory capacity. The connection type, weight value, and excitation mode of various nodes all influence how a neural network responds [23]–[25]. On the other hand, CNN is trained using a backpropagation algorithm, a supervised learning algorithm like a human brain. In our research, CNN consists of three convolutional layers that were used. Figure 6 describes our CNN model.

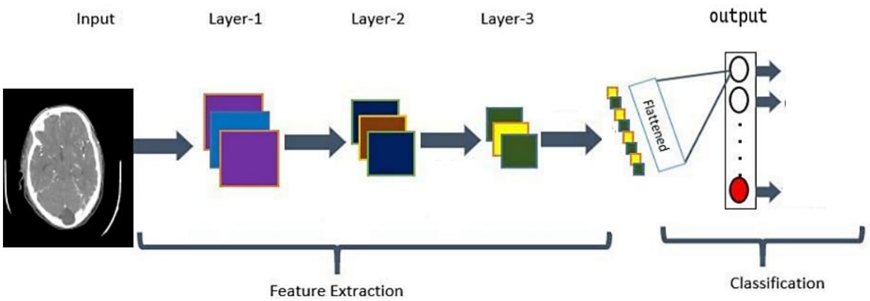

Figure 6. The architecture of our CNN model

3. CLASSIFICATION RESULTS AND PERFORMANCE EVALUATION

The classification process was carried out in two stages, the first of which was classified into two types: Normal (No hemorrhage) or abnormal (hemorrhage). The second stage was to classify hemorrhage into four types: epidural hemorrhage, subdural hemorrhage, intraventricular hemorrhage, and intraparenchymal hemorrhage. In both stages, four classification algorithms were applied: LR, KNN, SVM, and CNN.

3.1. Performance evaluation

To determine the classification performance, the evaluation employed the following performance metrics: i) area under the curve (AUC), ii) classification accuracy (CA), iii) F1-score, iv) Precision, and v) Recall. The AUC represents the area enclosed by the receiver operating characteristic (ROC) curve. A completely random classifier yields an AUC of 0.5, while an ideal classifier achieves an AUC of 1. The range of possible AUC values is from 0 to 1. However, if the AUC falls below 0.5, it indicates that by reversing the outputs of the classifier, a higher score can be obtained, suggesting an error in the classification process [26]. Classification accuracy (CA) is a straightforward measure that quantifies the ratio of correctly predicted observations to the total number of observations. Accuracy is a valuable metric for symmetric datasets where the occurrences of false positives and false negatives are roughly balanced [27].

$$Accuracy = \frac{TP+TN}{TP+TN+FP+FN} \tag{4}$$

The F1-score is a performance measure that combines precision and recall through a weighted average. By incorporating information about both false positives and false negatives, the F1-score offers a more comprehensive evaluation than accuracy alone. This is especially valuable when dealing with uneven class distributions. When there is a no table difference in the impact of false positives and false negatives, it is preferable to consider both precision and recall having a more accurate and comprehensive evaluation of the classifier's performance.

$$F - measure = \frac{2*Precision*Recall}{Precision+Recall} \tag{5}$$

Precision is computed as the proportion of accurately predicted positive observations divided by the total number of predicted positive observations. A higher precision value implies a lower false-positive rate, indicating that the classifier effectively identifies positive instances while minimizing misclassification.

$$Precision = \frac{TP}{TP+FP} \tag{6}$$

Recall, also known as sensitivity or true positive rate, is determined as the ratio of correctly predicted positive observations to the total number of observations in the actual positive class. It quantifies the classifier's ability to identify all positive instances within the dataset [28]–[30].

$$Sensitivity = \frac{TP}{TP+FN} \tag{7}$$

3.2. Classification using CNN

The results indicate that CNN achieved an accuracy (CA) of 0.826% for the first stage. While for the second stage of classification, CNN achieved an accuracy (CA) of 0.851%. The confusion matrices for the CNN algorithm are presented in Table 1 and Table 2.

Table 1. CNN confusion matrix for stage 1

CNN	Hemorrhage	No Hemorrhage
Hemorrhage	288	52
No Hemorrhage	69	271

Table 2. CNN confusion matrix for stage 2

CNN	Epidural	Intraparenchymal	Intraventricular	Subdural
Epidural	720	75	2	13
Intraparenchymal	75	561	0	174
Intraventricular	0	0	814	6
Subdural	19	165	1	625

3.3. Classification using SVM

The classification process was performed using SVM, and results show that the SVM achieved an accuracy (CA) of 0.834% for the first stage. While for the second stage of classification, the SVM achieved an accuracy (CA) of 0.849%. In order to envision the performance for two stages, the confusion matrices of the SVM classifier were defined as shown in Table 3 and Table 4.

Table 3. SVM confusion matrix for stage 1

SVM	Hemorrhage	No Hemorrhage
Hemorrhage	272	68
No Hemorrhage	45	295

Table 4. SVM confusion matrix for stage 2

SVM	Epidural	Intraparenchymal	Intraventricular	Subdural
Epidural	664	113	0	33
Intraparenchymal	111	326	1	372
Intraventricular	0	1	818	1
Subdural	41	167	3	599

3.4. Classification using LR

The classification process was performed here. The classification results point out that the LR realized an accuracy (CA) of 0.834% for the first stage. While for the second stage of classification, the LR achieved an accuracy (CA) of 0.741%. The cerebral hemorrhage classifications results are shown in Table 5 and Table 6 where the confusion matrix is used to envision the performance for two stages using LR classifier.

Table 5. Logistic regression confusion matrix for stage 1

LR	Hemorrhage	No Hemorrhage
Hemorrhage	280	60
No Hemorrhage	58	283

Table 6. Logistic regression confusion matrix for stage 2

LR	Epidural	Intraparenchymal	Intraventricular	Subdural
Epidural	729	66	2	13
Intraparenchymal	66	590	1	153
Intraventricular	1	2	812	5
Subdural	10	164	1	635

3.5. Classification using KNN

The results indicate that the KNN achieved an accuracy (CA) of 0.725% for the first stage, while for the second stage, the KNN closely achieved an accuracy of 0.662%. KNN demonstrated the lowest classification rate for both stages. The confusion matrices for the KNN algorithm are presented in Table 7 and Table 8.

Table 7. KNN confusion matrix for stage 1

KNN	Hemorrhage	No Hemorrhage
Hemorrhage	319	21
No Hemorrhage	166	174

Table 8. KNN confusion matrix for stage 2

KNN	Epidural	Intraparenchymal	Intraventricular	Subdural
Epidural	601	141	11	57
Intraparenchymal	134	461	12	203
Intraventricular	27	33	750	10
Subdural	85	374	10	341

The classification results in Table 9 for stage 1 show that both the SVM and neural CNN methods perform significantly better, with AUC values reaching 0.917 and 0.915, respectively. With a score of 0.905, the LR method also shows impressive performance. The results also showed that the SVM method had the highest precision and recall with values of 0.835 and 0.834, respectively. In contrast to the precision and recall values of 0.725, the KNN method performs less well in this case. Moreover, LR, SVM, and CNN reach the largest F1 measurement value of 0.826, 0.834, and 0.822, respectively, while KNN achieves the lowest F1 measurement value of 0.712.

Furthermore, the classification results for stage 2 show that both the SVM and CNN methods perform significantly well, with AUC values of 0.971 and 0.965, respectively. With a score of AUC equal to 0.919, the LR algorithm also performs effectively. On the other hand, CCN technique obtains the highest F1, precision and recall scores. In contrast, the KNN method performs the least well in this instance, with accuracy and recall scores of 0.662, respectively. Additionally, the study shows that CNN and SVM algorithms reach the greatest F1-measure values of 0.851 and 0. 849, respectively, while the KNN approach receives the lowest F1-measure value of 0.663.

Table 9. Comparison between classifiers results for both stages

Model	AUC		CA		F1		Precision		Recall	
	Stage 1	Stage 2	Stage 1	Stage 2	Stage 1	Stage 2	Stage 1	Stage 2	Stage 1	Stage 2
CNN	0.915	0.965	0.826	0.851	0.822	0.851	0.823	0.852	0.822	0.851
LR	0.905	0.919	0.834	0.741	0.826	0.734	0.826	0.736	0.826	0.741
SVM	0.917	0.971	0.834	0.849	0.834	0.849	0.835	0.849	0.834	0.849
KNN	0.866	0.882	0.725	0.662	0.712	0.663	0.775	0.671	0.725	0.662

3.6. Receiver operating characteristic

The Receiver operating characteristic (ROC) curve is used to show the overall performance of a diagnostic test by connecting the coordinate points with "1 - specificity" (= false positive rate) as the x-axis and "sensitivity" as the y-axis for all cut-off positions where the test results are measured [31]. It is also used to identify the best cut-off value for diagnosing diseases. The effectiveness of the suggested method was evaluated using the ROC, and the resultant curve for two stages is shown in Figure 7. Figure 7(a) show ROC of stage 1 and Figure 7(b) show ROC of stage 2.

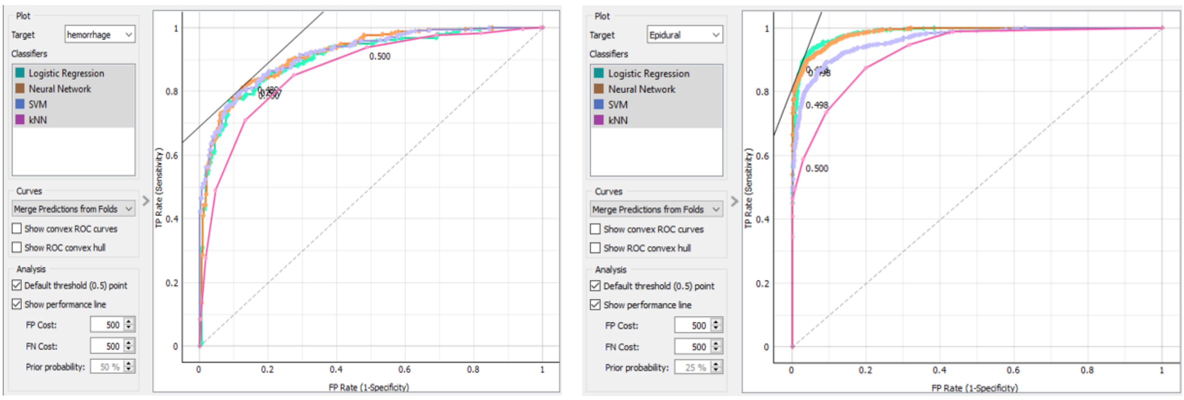

(a) (b)

Figure 7. Receiver operating characteristic (a) ROC of stage 1, (b) ROC of stage 2

The SVM algorithm achieves the maximum value of area under the curve (AUC: 0.917) for stage 1, followed closely by the CNN (AUC: 0.915) and LR (AUC: 0.905) approaches, according to Figure 8. With an AUC of 0.866, the KNN approach, in contrast, yields the least desirable outcome. For stage 2, the effectiveness of the suggested technique was also assessed as Figure 8 demonstrates that the SVM algorithm achieves the highest area value under the ROC curve (AUC: 0.971), closely followed by the CNN (AUC: 0.965) and LR (AUC: 0.919) methods. Conversely, the KNN method produces the least favorable result with an AUC of 0.882.

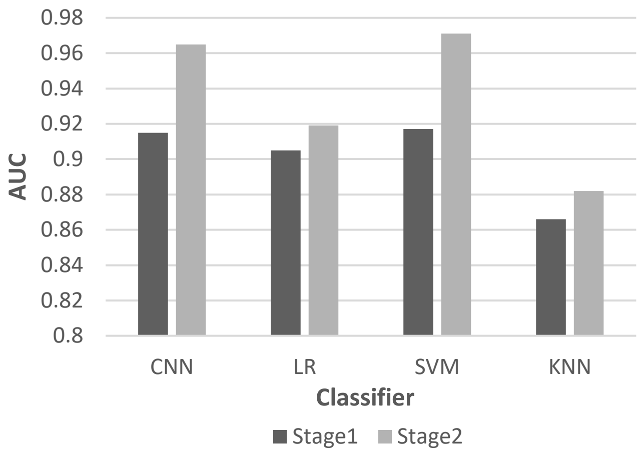

Figure 8. Area under the curve (AUC)

4. CONCLUSION

This study examines the mechanism of using several supervised classifiers to classify images using Orange3 data mining techniques. A dataset, which includes a total of 1,156 brain CT images, was obtained through Kaggle. The classification procedure using LR, CNN, SVM, and KNN, was divided into stage 1, images were classified into two categories (hemorrhage and no hemorrhage), and stage 2, images were classified into four categories (epidural, intraparenchymal, intraventricular, and subdural hemorrhage). According to the classification results, SVM performs most effectively in the stage 1 scenario according to classification accuracy, whereas CNN is more efficient in the stage 2 scenario. On the other hand, the KNN classifier performs poorly in both stages.

REFERENCES

[1] M. Ammar, M. A. Lamri, S. Mahmoudi, and A. Laidi, "Deep learning models for intracranial hemorrhage recognition: A comparative study," *Procedia Computer Science*, vol. 196, pp. 418–425, 2022, doi: 10.1016/j.procs.2021.12.031.

[2] J. A. Caceres and J. N. Goldstein, "Intracranial hemorrhage," *Emergency Medicine Clinics of North America*, vol. 30, no. 3, pp. 771–794, Aug. 2012, doi: 10.1016/j.emc.2012.06.003.

[3] T. D. Phong *et al.*, "Brain hemorrhage diagnosis by using deep learning," in *Proceedings of the 2017 International Conference on Machine Learning and Soft Computing (ICMLSC '17)*, Jan. 2017, pp. 34–39, doi: 10.1145/3036290.3036326.

[4] M. Rajagopal, S. Buradagunta, M. Almeshari, Y. Alzamil, R. Ramalingam, and V. Ravi, "An efficient framework to detect intracranial hemorrhage using hybrid deep neural networks," *Brain Sciences*, vol. 13, no. 3, Art. no. 400, Feb. 2023, doi: 10.3390/brainsci13030400.

[5] H. Chen, S. Khan, B. Kou, S. Nazir, W. Liu, and A. Hussain, "A smart machine learning model for the detection of brain hemorrhage diagnosis based internet of things in smart cities," *Complexity*, vol. 2020, pp. 1–10, Sep. 2020, doi: 10.1155/2020/3047869.

[6] A. Sage and P. Badura, "Intracranial hemorrhage detection in head CT using double-branch convolutional neural network, support vector machine, and random forest," *Applied Sciences*, vol. 10, no. 21, p. 7577, Oct. 2020, doi: 10.3390/app10217577.

[7] J. Nemcek, R. Jakubicek, and J. Chmelik, "Localization and classification of intracranial hemorrhages in CT data," in *IFMBE Proceedings*, Springer International Publishing, 2020, pp. 767–773. doi: 10.1007/978-3-030-64610-3_86.

[8] M. Okuyar and A. F. Kamanli, "Ischemia and hemorrhage detection in CT images with Hyper parameter optimization of classification models and Improved UNet segmentation model," *Sakarya University Journal of Computer and Information Sciences*, vol. 6, no. 1, pp. 48–58, Apr. 2023, doi: 10.35377/saucis...1259584.

[9] S. Gudadhe and A. Thakare, "Classification of intracranial hemorrhage CT images for stroke analysis with transformed and image-based GLCM features," *Research Square*, Jan. 2022, doi: 10.21203/rs.3.rs-1234293/v1.

[10] Kaggle, "Your machine learning and data science community," *Kaggle*, 2010. https://www.kaggle.com/ (accessed Nov 18, 2023).

[11] Z. Yang and D. Li, "Application of logistic regression with filter in data classification," *2019 Chinese Control Conference (CCC)*, Guangzhou, China, 2019, pp. 3755-3759, doi: 10.23919/chicc.2019.8865281.

[12] R. Jankovic Babic, "Classifying cultural heritage images by using decision tree classifiers in WEKA," In *Proceedings of the 1st international workshop on visual pattern extraction and recognition for cultural heritage understanding co-located with 15th Italian research conference on digital libraries (IRCDL 2019)*, Pisa, Italy. 2019, pp. 119-127.

[13] L. Pace, *Logistic regression. beginning r: An introduction to statistical programming*. 1st edition, Apress Berkeley, CA, Oct. 2012.

[14] Q. Bi, K. E. Goodman, J. Kaminsky, and J. Lessler, "What is machine learning? A primer for the epidemiologist," *American Journal of Epidemiology*, Oct. 2019, doi: 10.1093/aje/kwz189.

[15] E. Y. Boateng and D. A. Abaye, "A review of the logistic regression model with emphasis on medical research," *Journal of Data Analysis and Information Processing*, vol. 07, no. 04, pp. 190–207, 2019, doi: 10.4236/jdaip.2019.74012.

[16] M. Altayeb and A. Al-Ghraibah, "Classification of three pathological voices based on specific features groups using support vector machine," *International Journal of Electrical and Computer Engineering (IJECE)*, vol. 12, no. 1, pp. 946-956, Feb. 2022, doi: 10.11591/ijece.v12i1.pp946-956.

[17] B. X. W. Liew, F. M. Kovacs, D. Rügamer, and A. Royuela, "Machine learning versus logistic regression for prognostic modelling in individuals with non-specific neck pain," *European Spine Journal*, vol. 31, no. 8, pp. 2082–2091, Mar. 2022, doi: 10.1007/s00586-022-07188-w.

[18] A. Al-Ghraibah, M. Algharibeh, W. AlMohtasib, and M. Altayeb, "Classification of long bone x-ray images using new features and support vector machine," *International Journal of Advanced Trends in Computer Science and Engineering*, vol. 10, no. 3, pp. 1494–1500, Jun. 2021, doi: 10.30534/ijatcse/2021/011032021.

[19] S. Santhoshkumar, V. Varadarajan, S. Gavaskar, J. J. Amalraj, and A. Sumathi, "Machine learning model for intracranial hemorrhage diagnosis and classification," *Electronics*, vol. 10, no. 21, p. 2574, Oct. 2021, doi: 10.3390/electronics10212574.

[20] H. A. Owida, A. Al-Ghraibah, and M. Altayeb, "Classification of chest X-Ray images using wavelet and MFCC features and support vector machine classifier," *Engineering, Technology & Applied Science Research*, vol. 11, no. 4, pp. 7296–7301, Aug. 2021, doi: 10.48084/etasr.4123.

[21] Q. Lv, S. Zhang, and Y. Wang, "Deep learning model of image classification using machine learning," *Advances in Multimedia*, vol. 2022, pp. 1–12, Jul. 2022, doi: 10.1155/2022/3351256.

[22] J. Jiafeng and L. Yun, "Review of typical machine learning platforms for big data," *Journal of Computer Applications*, vol. 37, no. 11, p. 3039, Nov. 2017, doi: 10.11772/J.ISSN.1001-9081.2017.11.3039.

[23] K. Jnawali, M. R. Arbabshirani, N. Rao, and A. A. Patel, "Deep 3D convolution neural network for CT brain hemorrhage classification," in *Medical Imaging 2018: Computer-Aided Diagnosis*, Feb. 2018. doi: 10.1117/12.2293725.

[24] O. Ronneberger, P. Fischer, and T. Brox, "U-Net: Convolutional networks for biomedical image segmentation," in *Medical Image Computing and Computer-Assisted Intervention – MICCAI 2015*, Springer International Publishing, 2015, pp. 234–241. doi: 10.1007/978-3-319-24574-4_28.

[25] Y. Wu and J. Feng, "Development and application of artificial neural network," *Wireless Personal Communications*, vol. 102, no. 2, pp. 1645–1656, Dec. 2017, doi: 10.1007/s11277-017-5224-x.

[26] S. Talukdar *et al.*, "Land-use land-cover classification by machine learning classifiers for satellite observations—a review," *Remote Sensing*, vol. 12, no. 7, p. 1135, Apr. 2020, doi: 10.3390/rs12071135.

[27] S. Uddin, I. Haque, H. Lu, M. A. Moni, and E. Gide, "Comparative performance analysis of K-nearest neighbour (KNN) algorithm and its different variants for disease prediction," *Scientific Reports*, vol. 12, no. 1, Apr. 2022, doi: 10.1038/s41598-022-10358-x.

[28] A. Tharwat, "Classification assessment methods," *Applied Computing and Informatics*, vol. 17, no. 1, pp. 168–192, Jan. 2021, doi: 10.1016/j.aci.2018.08.003.

[29] J. Dey, M. S. Bin Hossain, and M. A. Haque, "An ensemble SVM-based approach for voice activity detection," Dec. 2018. doi: 10.1109/icece.2018.8636745.

[30] B. Sabir, F. Rouda, Y. Khazri, B. Touri, and M. Moussetad, "Improved algorithm for pathological and normal voices identification," *International Journal of Electrical and Computer Engineering (IJECE)*, vol. 7, no. 1, p. 238, Feb. 2017, doi: 10.11591/ijece.v7i1.pp238-243.

[31] K. Hajian-Tilaki, "Receiver operating characteristic (ROC) curve analysis for medical diagnostic test evaluation.," *Caspian journal of internal medicine*, vol. 4, no. 2, pp. 627–635, 2013.

BIOGRAPHIES OF AUTHORS

Areen Arabiat earned her BSc in computer engineering in 2005 from Al Balqaa Applied University (BAU), and her MSc in intelligent transportation systems (ITS) from Al Ahliyya Amman University (AAU) in 2022. Her thesis was about "Traffic congestion prediction using machine learning Amman City: case study". She is currently a computer lab supervisor at the Faculty of Engineering in Al-Ahliyya Amman University (AAU) since 2013. Her research interests are focused on the following areas: machine learning, data mining, and artificial intelligence. She can be contacted at email: a.arabiat@ammanu.edu.jo.

Muneera Altayeb obtained a bachelor's degree in computer engineering in 2007, and a master's degree in communications engineering from the University of Jordan in 2010. She has been working as a lecturer in the Department of Communications and Computer Engineering at Al-Ahliyya Amman University since 2015, in addition to her administrative experience as assistant dean of the Faculty of Engineering during the period (2020-2023). Her research interests focus on the following areas: digital signals and image processing, machine learning, robotics, and artificial intelligence. She can be contacted at email: m.altayeb@ammanu.edu.jo.